3D VISUALIZATION OF 'REAL' GRAPHENE IN NANOCOMPOSITE AND THE RELATED MICROMECHANICS

Zheling Li[1], Xinyu Ma[2], Yingjie`Yu[3], Thomas J. A. Slater[4], Robert J. Young[5], Timothy L. Burnett[6]

[1]National Graphene Institute/School of Materials, Oxford Road, Manchester, UK M13 9PL
Email: zheling.li@manchester.ac.uk
[2]Henry Moseley X-ray Imaging Facility/School of Materials, Oxford Road, Manchester, UK M13 9PL
Email: xinyu.ma@postgrad.manchester.ac.uk
[3]National Graphene Institute/School of Materials, Oxford Road, Manchester, UK M13 9PL
Email: yingjie.yu@student.manchester.ac.uk
[4]Henry Moseley X-ray Imaging Facility/School of Materials, Oxford Road, Manchester, UK M13 9PL
Email: thomas.slater-2@manchester.ac.uk
[5]National Graphene Institute/School of Materials, Oxford Road, Manchester, UK M13 9PL
Email: robert.young@manchester.ac.uk
[6]Henry Moseley X-ray Imaging Facility/School of Materials, Oxford Road, Manchester, UK M13 9PL
Email: timothy.burnett@manchester.ac.uk

Keywords: Graphene, Nanocomposites, X-ray computed tomography, micromechanics

Abstract

Graphene has huge potential in composite applications, and it enables the composites not only good mechanical but also multifunctionality. Similar to the conventional composites, the graphene with higher degree of orientation,[10] larger lateral dimension and higher aspect ratio tends to give better reinforcement. However, the characterisation methods of graphene and other nanofillers are not as rich as that for micro-scale fibres. Scanning electron microscopy, atomic force microscopy and transmission electron microscopy can be employed to reveal the morphology of graphene, but they are usually carried out before the fillers being mixed with the matrix thus it fails to identify the damage during the composites processing.

In this work, the epoxy nanocomposites with different loadings of graphene nanoplatelets (GNP) are prepared. The X-ray computed tomography (CT) is used to identify and resolve individual GNP flake in the nanocomposites. It is found that the GNPs have variable geometry, defects density, waviness, number of layers and the agglomeration, all of which will have significant impact on enhancing the mechanical properties of the nanocomposites. This is thought to be the reason why the micromechanics models often misestimate the Young's modulus of the nanocomposites.

1. Introduction

Graphene has shown its huge potential in the application of composites [4], on enhancing mechanical [12], electrical and thermal properties [4]. For fibre composites, it is known that the fibre diameter [17], length [6], orientation [1] etc. all determine the mechanical properties of the composites. However, the characterisation of the physical properties of nanomaterials, such as graphene is quite limited. Some attempts have been made as reported from Hu et al.[5], Paton et al.[14], but it was prior to the composites processing, after which it will inevitably change. Additionally, other physical properties like the fracture, wrinkling and the reagglomeration of the graphene are very difficult to visualize in the nanocomposites [2, 13]. A reliable and clear way of visualizing the graphene flakes are still of great importance to explain the micromechanics of graphene reinforced nanocomposites [11, 15]. Recent work has demonstrated the use of X-ray CT scan to observe graphene nanoplatelets

(GNP), but a more careful examination of the morphology and structure of the individual GNP flakes in more detail is still needed [8].

In this work, the epoxy nanocomposites with different loadings of GNP are prepared. The X-ray CT is used to identify massive number of GNPs in the nanocomposites and resolve the individual GNP flake. It is found that the GNPs have variable geometry, defects density, waviness, number of layers and the agglomeration. Different features of the GNP have been identified, all of which play significant roles in determining the mechanical properties of the nanocomposites, and this is thought to be the reason why the micromechanics models often overestimate the Young's modulus of the nanocomposites. In contrast, the information resolved by X-ray CT on individual GNP flakes delivers a more accurate estimation of mechanical properties of GNP nanocomposites.

2. Experimental

2.1 Materials

The GNP powder was Grade M-25 supplied by XG Science (Michigan, USA). The epoxy resin and hardener were Araldite LY and Aradur 5052 (Huntsman).

2.2 Sample Preparation

The neat epoxy and nanocomposites with different GNP loadings of 0.1 wt%, 0.5 wt%, 1 wt% and 1.5 wt% have been prepared as described previously [16].

2.3 Characterisation

The tensile test was carried out by using an Instron 4301 machine and the size of the specimens follows ASTM D638 Type IV, in a conditioned laboratory. The samples for X-ray CT were prepared by using a microtome (Leica Ultracut UC6 Ultramicrotome) into a pyramid shape with the cross area of top less than 0.1 mm x 0.1 mm. The data were collected by the Zeiss Xradia Ultra 810 instrument with a source energy 5.5 keV. The projections are acquired by phase contrast mode. After the projections, the data is reconstructed using a filtered back projection reconstruction through the Zeiss XMRecontrutor software. Data was then visualized and quantified using Avizo software package (version 9.2.0).

3. Results and Discussion

Two typical GNP flakes are shown in Figure 1a and b, and it can be found that even from the same batch of GNP, the lateral dimension varies significantly, which can be quantified by the size factor η_l as calculated in [18]:

$$\eta_l = 1 - \frac{\tanh\left(n/2 \cdot s\right)}{n/2 \cdot s} \tag{1}$$

where s is the aspect ratio of the flake. $n=[G_m/E_{gra} \cdot V_{gra}/(1-V_{gra})]^{1/2}$ is a measure of the interfacial stress transfer efficiency, where G_m is the shear modulus of the polymer matrix. Further details can be found in Ref.[3, 18]. The corresponding s and η_l of the two flakes are shown in Figure 1c according to Eq.1. Different flake sizes lead to significant values of η_l, and even within one flake, s is not a constant that it is smaller near the edge than that in the middle of the flake. Additionally, a line defect can be seen as highlighted by the blue circle in Figure 1b which possibly leads to the fracture (highlighted by the yellow circle) of the GNP flake. Both of these damage the structural integrity of the flake, or lead to further fracturing of the flake, thus reduces s and η_l, very likely during the sample preparation. Schematic diagrams of the issues discussed above are shown in Figure 1.

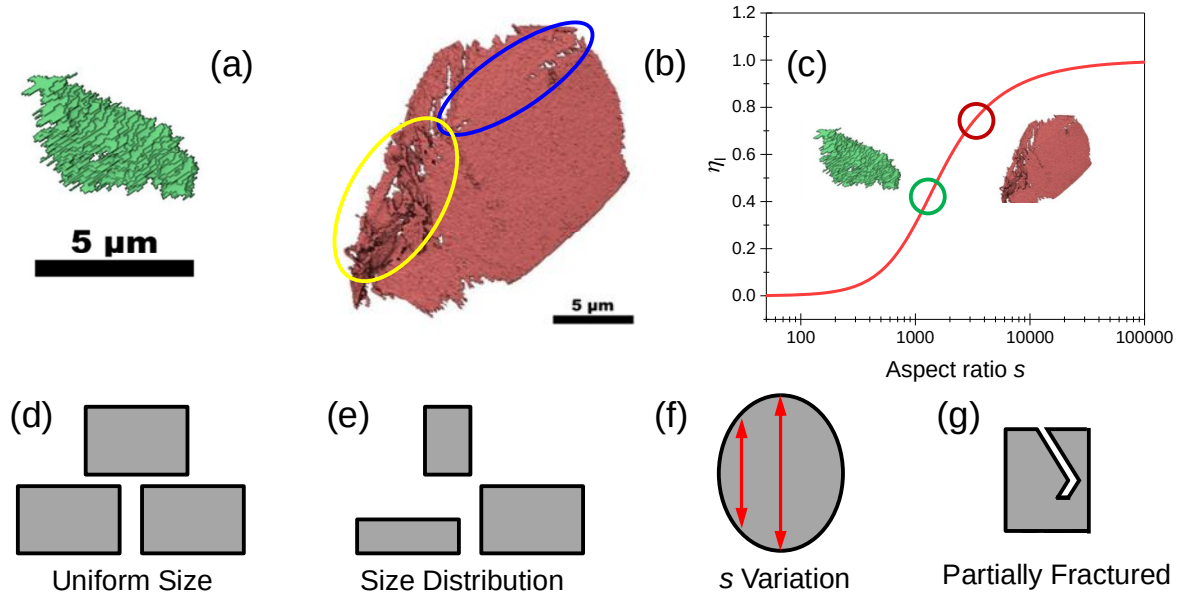

Figure 1 (a) Small GNP flake. (b) GNP flake with line defect and damaged edge. (c) η_l as the function of *s*. The η_l of the flakes in (a) and (b) are indicated. Schematic illustration of (d) uniform size, (e) non-uniform size, (f) the variation of *s* in one flake and (g) partially fractured flake.

As X-ray CT technique can measure the surface area of the GNP flakes, it can also be used to calculate the real lateral dimension of GNP flakes in composites statistically which can be used to precisely estimate the mechanical properties of GNP nanocomposites. The distribution of the GNP flakes size, assuming flakes are square, and the corresponding size factor η_l calculated according to Eq.1 is shown in Figure 2a. It can be found that most of the GNP flakes have a quite small lateral dimension while only a few big ones with large size. The average GNP flake size is further used to calculate the Young's modulus of nanocomposites using the rule of mixture as:

$$E_c = \eta_o E_{gra} \cdot \eta_l V_{gra} + E_m \left(1 - V_{gra}\right) \quad (2)$$

where E_c and E_m are the Young's modulus of the composite and matrix, respectively. E_{gra} is the Young's modulus of graphene [7] and V_{gra} is the volume fraction of GNP (vol%) that can be converted from wt% according to Ref.[9]. η_o is the Krenchel orientation factor, taken as 8/15. The calculated values are shown as gray line in 错误！未找到引用源。b. It can be seen that the estimation using the average flakes size does not fit with the experimental E_c data (blue points).

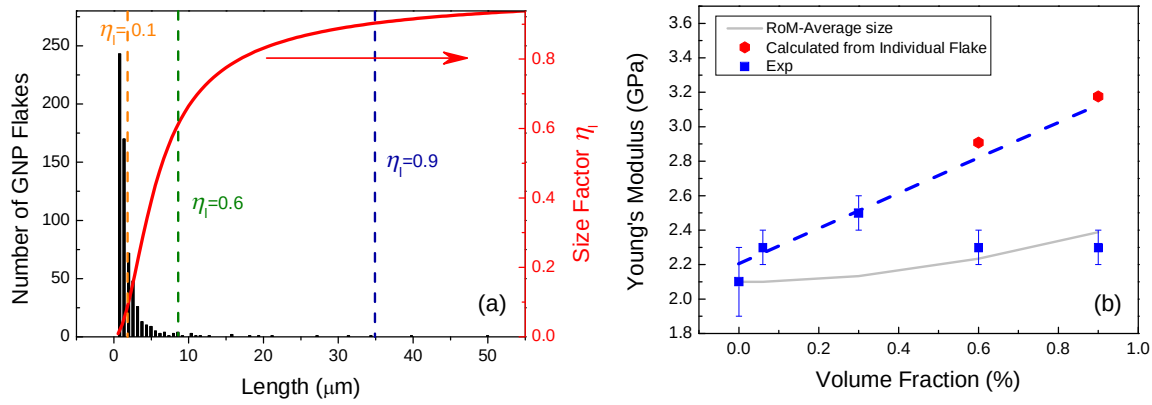

Figure 2 (a) The distribution of the GNP flakes size and the corresponding calculated length factor η_l. (b) The calculated Young's modulus by average flake size (grey line) and from individual GNP flake (red points), and the experimental E_c (blue points).

However, the use of X-ray CT enables a detailed estimation of the Young's modulus by taking into account the contribution of each flake individually. If the length factor η_l is considered individually for each flake from the actual size resolved by X-ray CT, the E_c can be re-calculated as the red points in Figure 2b. It can be seen they are on the linear fit line of the experimental data at lower GNP concentration. The deviation at higher GNP concentration is speculated to be due to the agglomeration at higher GNP loading.

4. Conclusion

A nanocomposite has been prepared by mixing GNP with epoxy resin with different GNP loadings. It has been demonstrated that the use of nanoscale X-ray CT enables the visualization of the 'real' structure, such as morphology, defects and reagglomeration of the GNP in nanocomposties. Different from the conventional analysis using the average GNP flakes size, the use of X-ray CT enables a calculation of the mechanical property of nanocomposites based on the data on individual GNP flakes, which show a better fit to the experimental results.

References

[1] M.C. Andrews, R.J. Day, X. Hu, R.J. Young. Dependence of fibre strain on orientation angle for off-axis fibres in composites. *Journal of Materials Science Letters*, 11:1344-1346, 1992.

[2] S. Chandrasekaran, N. Sato, F. Tölle, R. Mülhaupt, B. Fiedler, K. Schulte. Fracture toughness and failure mechanism of graphene based epoxy composites. *Composites Science and Technology*, 97:90-99, 2014.

[3] L. Gong, I.A. Kinloch, R.J. Young, I. Riaz, R. Jalil, K.S. Novoselov. Interfacial stress transfer in a graphene monolayer nanocomposite. *Advanced Materials*, 22:2694-2697, 2010.

[4] K. Hu, D.D. Kulkarni, I. Choi, V.V. Tsukruk. Graphene-polymer nanocomposites for structural and functional applications. *Progress in Polymer Science*, 39:1934-1972, 2014.

[5] L.-H. Hu, F.-Y. Wu, C.-T. Lin, A.N. Khlobystov, L.-J. Li. Graphene-modified lifepo4 cathode for lithium ion battery beyond theoretical capacity. *Nature Communications*, 4:1687, 2013.

[6] Y. Huang, R.J. Young. Interfacial micromechanics in thermoplastic and thermosetting matrix carbon fibre composites. *Composites Part A: Applied Science and Manufacturing*, 27:973-980, 1996.

[7] C. Lee, X. Wei, J.W. Kysar, J. Hone. Measurement of the elastic properties and intrinsic strength of monolayer graphene. *Science*, 321:385-388, 2008.

[8] S. Li, Z. Li, T.L. Burnett, T.J.A. Slater, T. Hashimoto, R.J. Young. Nanocomposites of graphene nanoplatelets in natural rubber: Microstructure and mechanisms of reinforcement. *Journal of Materials Science*, 52:9558-9572, 2017.

[9] Z. Li, R.J. Young, I.A. Kinloch. Interfacial stress transfer in graphene oxide nanocomposites. *ACS Applied Materials & Interfaces*, 5:456-463, 2013.

[10] Z. Li, R.J. Young, N.R. Wilson, I.A. Kinloch, C. Vallés, Z. Li. Effect of the orientation of graphene-based nanoplatelets upon the young's modulus of nanocomposites. *Composites Science and Technology*, 123:125-133, 2016.

[11] J. Liang, Y. Huang, L. Zhang, Y. Wang, Y. Ma, T. Guo, Y. Chen. Molecular-level dispersion of graphene into poly(vinyl alcohol) and effective reinforcement of their nanocomposites. *Advanced Functional Materials*, 19:2297-2302, 2009.

[12] D.G. Papageorgiou, I.A. Kinloch, R.J. Young. Mechanical properties of graphene and graphene-based nanocomposites. *Progress in Materials Science*, 90:75-127, 2017.

[13] Y.T. Park, Y. Qian, C. Chan, T. Suh, M.G. Nejhad, C.W. Macosko, A. Stein. Epoxy toughening with low graphene loading. *Advanced Functional Materials*, 25:575-585, 2015.

[14] K.R. Paton, E. Varrla, C. Backes, R.J. Smith, U. Khan, A. O'Neill, C. Boland, M. Lotya, O.M. Istrate, P. King, T. Higgins, S. Barwich, P. May, P. Puczkarski, I. Ahmed, M. Moebius, H. Pettersson, E. Long, J. Coelho, S.E. O'Brien, E.K. McGuire, B.M. Sanchez, G.S. Duesberg, N. McEvoy, T.J. Pennycook, C. Downing, A. Crossley, V. Nicolosi, J.N. Coleman. Scalable production of large quantities of defect-free few-layer graphene by shear exfoliation in liquids. *Nature Materials*, 13:624-630, 2014.

[15] J. Shang, Y. Chen, Y. Zhou, L. Liu, G. Wang, X. Li, J. Kuang, Q. Liu, Z. Dai, H. Miao, L. Zhi, Z. Zhang. Effect of folded and crumpled morphologies of graphene oxide platelets on the mechanical performances of polymer nanocomposites. *Polymer*, 68:131-139, 2015.

[16] C. Vallés, F. Beckert, L. Burk, R. Mülhaupt, R.J. Young, I.A. Kinloch. Effect of the c/o ratio in graphene oxide materials on the reinforcement of epoxy-based nanocomposites. *Journal of Polymer Science Part B: Polymer Physics*, 54:281-291, 2016.

[17] K. Young, F.M. Blighe, J.J. Vilatela, A.H. Windle, I.A. Kinloch, L. Deng, R.J. Young, J.N. Coleman. Strong dependence of mechanical properties on fiber diameter for polymer−nanotube composite fibers: Differentiating defect from orientation effects. *ACS Nano*, 4:6989-6997, 2010.

[18] R.J. Young, M. Liu, I.A. Kinloch, S. Li, X. Zhao, C. Vallés, D.G. Papageorgiou. The mechanics of reinforcement of polymers by graphene nanoplatelets. *Composites Science and Technology*, 154:110-116, 2018.